THE HOPKINS ULTRAVIOLET TELESCOPE HANDBOOK

Version 1.1

October 1993

Prepared by:
Samuel T. Durrance, Gerard A. Kriss, and William P. Blair

Arthur F. Davidsen
Principal Investigator

Center for Atrophysical Sciences
The Johns Hopkins University

PREFACE

NOTE: Parts of this handbook may no longer apply to the data in MAST, because they are in a different format and processed with an updated pipeline. This document is maintained primarily for information about the mission and hardware. Users are encouraged to read the paper by Dixon et al. *PASP*, 2013 for updatedinformation on the calibration and processing of the data now available on MAST.

The HUT Instrument Handbook is intended to serve a variety of functions, from aiding guest investigators in writing proposals to serving as a general reference for successful guest investigators, new team members, and the flight crew. As a result, different readers will want to concentrate on specific sections to accomplish their primary objectives. This handbook will be updated in future revisions to reflect new calibration data and actual flight performance for HUT on Astro-2.

The introduction gives a succinct description of HUT and its capabilities that will be of use to all readers. For those planning to write observing proposals, the introduction and section 5, describing feasibility estimates, will prove most useful. The article ``The Hopkins Ultraviolet Telescope: Performance and Calibration during the Astro-1 Mission'' by Davidsen et al. (ApJ, 392, 264-271, 1992 June 10) is also recommended reading. Proposers who push the capabilities of the telescope at either the faint end or the bright end should consult section 4 on calibration to gain a better sense of what is possible and what may be difficult. If there is any question about HUT's capabilities, do not hesitate to consult with Dr. William P. Blair, who is serving as the interim HUT Guest Investigator support contact at Johns Hopkins University (phone: 410/516-8447; email: wpb@pha.jhu.edu), for more detailed explanations.

Successful guest investigators, new team members, and the flight crew are urged to read the whole handbook for a comprehensive view of HUT and its operation both in orbit and on the ground. For users who will be directly associated with HUT operations, sections 2 and 3 describing the hardware and its operation will be most valuable. For team members participating in science planning, section 3 on operations, and section 6 on mission planning provide the best background. For users of HUT data, either from Astro-1 or Astro-2, section 4 on calibration and section 5 on making observational feasibility estimates contain the most pertinent information. The handbook will probably not answer all questions that a user might have, but will refer the reader to the appropriate reference document for the pertinent details.

Reprints of articles based on HUT Astro-1 data which were accepted for publication before the end of 1992 have been collected in a book, Scientific Results from the Hopkins Ultraviolet Telescope (ed. A. F. Davidsen), which is available on request. (Call Sharon K. Busching at 410-516-5367, or send electronic mail to skb@pha.jhu.edu).

Next Up Previous Contents

Next: Contents

6/23/1999

Contents

List of Figures

List of Tables

INTRODUCTION

The Hopkins Ultraviolet Telescope (HUT) is one of three major instruments that comprise the Astro Observatory. It mounts on the Spacelab Instrument Pointing System (IPS) along with the Ultraviolet Imaging Telescope (UIT) and the Wisconsin Ultraviolet Photo-Polarimeter Experiment (WUPPE). The observatory is attached to the cargo bay of the Space Shuttle on two Spacelab pallets. All three instruments are operated as a single observatory. The Astro Observatory mounted in the Shuttle as it will be configured for Astro-2 is shown in Figure 1-1.

Figure 1-1: The Astro Observatory mounted in the Shuttle as it will be configured for Astro-2.

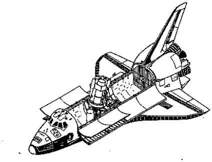

Table 1-1: HUT Instrument Design Characteristics for Astro-2

Telescope	
Prime Focus Paraboloid	
Aperture	90 cm
Collecting Area	5120 cm^2
Focal Ratio	$f/2$
Plate Scale	115″ mm^{-1}
	8.7 μm $('')^{-1}$
Mirror Coating	Silicon Carbide
Spectrograph	
Concave Grating, Rowland Circle Design	
Grating Diameter	200 mm
Radius of Curvature	400 mm
Groove Density	600 lines mm^{-1}
Coating	Silicon Carbide
Dispersion	41.5 Å mm^{-1}
Wavelength Coverage	
—First Order	814–1876 Å
—Second Order	407–938 Å
Detector	
Microchannel Plate Intensified Linear Photodiode Array (Pulse-Counting)	
Photocathode	Cesium Iodide
Active Length	25 mm
Diode Size	25 $\mu m \times 2.5$ mm
	($\sim$ 1 Å $diode^{-1}$)
Number of Diodes	1024
Spectrograph Resolution	75 μm
—First Order	$\sim$ 3 Å
—Second Order	$\sim$ 1.5 Å
Time Resolution	1 ms in high time mode
	2 s in histogram mode
Absolute Timing	3 ms
Maximum Event Rate (point source)	
—Across Array	5000 cts s^{-1}
—Emission Lines	20 cts $Å^{-1}$ s^{-1}
Dark Count Rate	0.001 cts $Å^{-1}$ s^{-1}

The HUT is an instrument designed for moderate-resolution (R = 300) spectrophotometry of faint astronomical objects ($m_v \lesssim 6$) at far- and extreme-ultraviolet wavelengths (415-1860 Å) with special emphasis on the region between Lyman-α (1216 Å) and the Lyman limit (912 Å). Its principal elements are a 90 cm *f*/2 prime focus telescope, a normal incidence concave grating spectrograph, a microchannel plate detector, an integrating SIT vidicon field acquisition camera, and a dedicated experiment processor (DEP) for instrument control and data handling, including video processing, as well as a spectrometer processor (SP) that interfaces with the detector. Spectra are recorded in 2048 channels in a pulse-counting mode with a time resolution of 1 msec, except for the brightest sources where the time resolution is 2 sec. A conceptual diagram of HUT is given in Figure 1-21 and the instrument characteristics are summarized in Table 1-1. A description of the performance and calibration of HUT during the Astro-1 mission is given by Davidsen et al. (1992).

Figure 1-2: Drawing of the Hopkins Ultraviolet Telescope (plan view). Overall dimensions are 3.8m × 1.1m (diameter). Many of the principal components are labeled. Power supplies, computers, etc. are located in a separate electronics module, not shown.

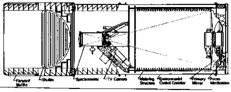

The HUT interfaces to the Shuttle through the Spacelab avionics. The avionics, which include computers, tape drives, and other electronic components needed for experiment control and data handling, is mounted on two pallets and inside a pressurized container called the Igloo. The Astro telescopes are mounted on a cruciform structure which is attached to the Instrument Pointing System (IPS). The IPS provides a stable pointing platform for the observatory; it is used to acquire and track targets of interest. The Payload Specialist (PS) views target fields imaged by the HUT acquisition camera on the Shuttle TV system. Using this image, a detailed finding chart, and the expected locations of up to three guide stars that are marked in the video image by the HUT DEP, the PS acquires the desired targets. Spectral data and video images are sent to the ground and displayed on the Telemetry Experiment Ground Support Equipment (TEGSE) at the Payload Operations Control Center (POCC) in real time for evaluation by the experimenters. The PS will normally control HUT from the Shuttle aft flight deck, but the experimenters in the POCC can also change instrument parameters and modify observing sequences by uplinking commands.

The instrument consists of two packages: the telescope module (TM), which contains the optics, spectrometer, and detector system within an environmental control canister (ECC); and the electronics module (EM), which contains the two experiment processors (the DEP and the SP) and other electronics necessary for thermal control and mechanism operations. The location of the hardware on the cruciform structure which is used to attach the instruments to the IPS is shown in Figure 1-3. A more detailed description of the hardware, its operation, and calibration will follow.

Figure 1-3: (a) The telescope module (TM) mounted on the cruciform;
(b) The HUT electronics module (EM) and other systems mounted on the integrated radiator system (IRS).

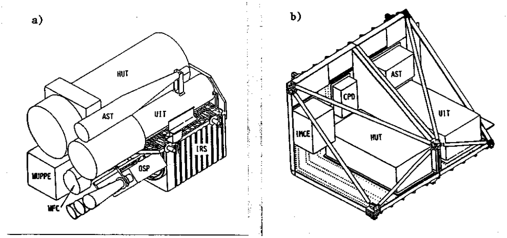

Next Up Previous Contents
Next: HARDWARE **Up:** No Title **Previous:** List of Tables

6/23/1999

HARDWARE

The HUT telescope module is attached to the Astro cruciform by means of kinematic mounts that are configured to maintain co-alignment with the other Astro instruments. The HUT electronics module is located on the integrated radiator system (IRS) to provide efficient rejection of heat generated by the electronic components. The IRS is also mounted on the cruciform structure with the other instruments. The HUT optics, spectrometer, and detector are all contained in a structure that consists of an environmental control canister (ECC), a shutter door assembly, and a forward baffle section as shown in Figure 2-1. The forward baffle section, located at the front of the ECC, acts as a light baffle and thermal transition element. The shutter doors provide for protection against contamination and excessive light levels and can allow for the observation of bright sources by restricting the aperture. The ECC provides for contamination protection and the maintenance of a stable thermal environment. The principal elements contained within the ECC are the primary mirror and mirror cell, the metering cylinder and spider arms, the spectrometer, the detector, and the acquisition TV camera. They are shown in Figure 2-2 and are described below.

Figure 2-1: The HUT optics, spectrometer, and detector are all contained in a structure that consists of an environmental control canister (ECC), a shutter door assembly, and a forward baffle section.

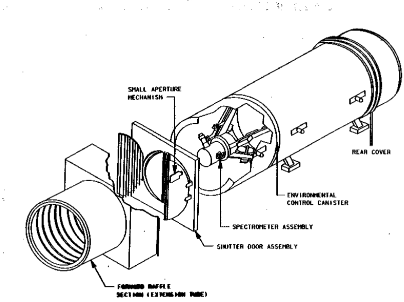

Figure 2-2: The principal elements contained within the ECC are the primary mirror and mirror cell, the metering cylinder and spider arms, the spectrometer, the detector, and the acquisition TV camera.

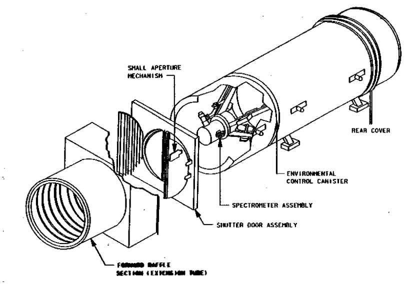
SMALL APERTURE
MECHANISM
REAR COVER
ENVIRONMENTAL
CONTROL CANISTER
SPECTROMETER ASSEMBLY
SHUTTER DOOR ASSEMBLY

Primary Mirror

For the Astro-1 flight, the primary mirror was made of Zerodur, which has a very low thermal expansion coefficient ($\alpha = 0.7 \times 10^{-7}$ ° C^{-1}). It is a 90 cm *f*/2 parabola that has been lightweighted by grinding material off the back. A cross section of the mirror is shown in Figure 2-3. The mirror was figured to provide 90$\%$ of the encircled energy within 1$''$ and was coated with iridium for high reflectivity in the ultraviolet. It is supported in the primary mirror cell by a clamping structure as shown in Figures 2-2 and 2-3. The mirror clamp is then attached to the mirror cell by three linear actuators (called the focus mechanisms) that can be used to focus and align the HUT optics. The mirror cell, the mirror clamp, and the focus mechanisms are all made of INVAR which also has a low thermal expansion coefficient ($\alpha = 7 \times 10^{-7}$ ° C^{-1}).

Figure 2-3: The HUT primary mirror shown with its clamping structure attached to the mirror cell assembly by the focus mechanism.

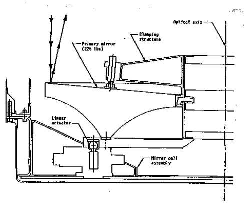

For Astro-2, the far-UV throughput of the telescope has been significantly improved by using a Cer-Vit mirror coated with silicon carbide over iridium. The physical characteristics of this mirror (which was the backup mirror for Astro-1) are nearly identical to the original flight mirror, but the SiC coating placed over the iridium improves the far-UV reflectivity by a factor of ~ 2. Unfortunately, the EUV response below 600 Å is considerably less.

If needed, the HUT primary mirror can be tilted to achieve co-alignment with the WUPPE experiment or for observing offset positions up to $\sim$ 2$'$ away. Normally, the WUPPE secondary mirror will be tilted for co-alignment, since the off-axis optical aberrations are less severe for WUPPE than for HUT. To focus or align HUT, the primary mirror along with its clamping structure can be moved, as a whole, fore and aft along the optical axis, or tilted. Each of the focus mechanisms is powered individually by a motor which drives a linear actuator fixed to the primary mirror clamp assembly. A single 400 Hz inverter, located in the EM, drives all the HUT mechanisms and can operate up to three at the same time if they are moving in the same direction (forward or reverse). The linear actuation of the focus mechanisms is accomplished by a differential screw assembly.

Control of the motors is furnished by the DEP, which is located in the EM. Position sensing potentiometers mounted on the gears of the differential screw mechanisms provide the DEP with the position of each mechanism. The software provides for various modes of mirror motion, all of which rely on a calculation of the run-time for each motor to accomplish a given motion. When a commanded motion is completed, the potentiometers are checked to determine if the correct position has been reached. An error message is issued if any one of the mechanisms is off by more than a preset lower limit (4 μm).

Using a stellar image placed near the center of the HUT TV camera, the crew will focus the telescope by commanding the primary mirror to move fore and aft. The mirror can also be automatically offset, scanned, or rastered during an observation by placing the necessary information in a sequence file. The observation sequence files will be discussed later.

Metering Structure

The metering structure, which consists of the metering cylinder and the spider arm assembly, is designed to attach the spectrometer to the mirror cell and maintain its position with sufficient accuracy to assure proper focus and alignment. It is constructed of INVAR to minimize the effects of temperature variations. The metering cylinder has a series of light baffles mounted on the inside to reduce scattered light. Various high voltage power supplies and the HUT TV camera are mounted on the spider arms in positions where they block the least amount of incoming light. The relationship between the metering structure and the other components of the telescope can be seen in Figures 1-2 and 2-2.

6/23/1999

Spectrometer

The spectrometer, shown in Figure 2-4, consists of a stainless steel vacuum housing, an entrance aperture wheel assembly, a stainless steel diffraction grating, a photon counting microchannel plate detector, a reference calibration lamp, and two redundant vacuum ion pumps. The spectrometer housing is fabricated of stainless steel to produce a clean vacuum environment and a stable, passive thermal design. Because its thermal expansion coefficient ($\alpha - 1.7 \times 10^{-5}$ ° C^{-1})is considerably higher than that of the INVAR metering structure, the location of the mounting ring on the spectrometer was chosen such that the different thermal expansion rates of the stainless steel housing and the INVAR metering structure produce no net change in the location of the spectrometer entrance aperture relative to the primary mirror over the operating temperature range of the telescope.

Figure 2-4: The spectrometer consists of a stainless steel vacuum housing, an entrance aperture wheel assembly, a stainless steel diffraction grating, a photon counting microchannel plate detector, a reference calibration lamp, and two redundant vacuum ion pumps.

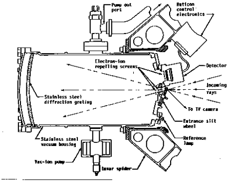

6/23/1999

Aperture Wheel Assembly

The aperture wheel assembly consists of a housing, a drive motor with reduction gearing, a mechanical geneva mechanism for indexing the wheel, and an aperture wheel. Only the wheel is shown in cross section in Figure 2-4. The aperture wheel is made of titanium and has a thin disk of nickel-plated copper mounted to its upper surface. There are eight positions, seven of which contain accurately etched holes to admit light into the spectrometer and one of which has no hole to provide a vacuum seal. The aperture positions and sizes for the Astro-2 configuration of HUT are given in Table 2-1.

Table 2-1: Spectrometer Aperture Wheel Positions

Aperture Position	Astro-1 Apertures Size (″)	Astro-1 Apertures Filter Type	Astro-2 Apertures Size (″)	Astro-2 Apertures Filter Type	Comments
0	Blank	—	Blank	—	Sealed position
1	29.6 diameter	—	12 diameter	—	
2	9.4 x 116	—	32 diameter	—	
3	30.0 diameter	Al	32 diameter	Al	
4	174 diameter	—	163 diameter	—	Calibration only
5	17 x 116	CaF_2	19 x 197	—	
6	17 x 116	—	10 x 56	—	
7	17 diameter	—	20 diameter	—	

The axis of the wheel is tilted 22.5^0 to the optical axis of the telescope. The nickel surface of the disk is optically smooth so that the image of the field surrounding the source is reflected into the TV camera, which is mounted on one of the spider arms at 45^0 to the optical axis of the telescope. The geneva mechanism uses approximately one half of a drive wheel cycle to rotate the wheel 45^0 and the remaining drive wheel cycle to unclamp and reclamp the aperture wheel to provide a vacuum seal for the spectrometer. The nominal time to move one aperture position is 25.6 sec. The final position of the wheel is dependent solely on mechanical tolerances of the geneva mechanism. The accuracy of placement is $\sim \pm 0.6''$ projected onto the sky or $\pm 5\ \mu$m in the focus direction. The position of the center of each aperture, in TV camera coordinates, is maintained in the DEP memory. For the purpose of target acquisition, a fiducial mark representing the aperture to be used during an observation is generated by the DEP and placed in the video image. There is a small amount of backlash in the drive motor gearing which must be accounted for by the DEP when generating the location of the aperture.

Diffraction Grating

The diffraction grating is fabricated out of stainless steel so that its radius of curvature will expand and contract at the same rate as the spectrometer housing and thus maintain proper focus. The grating characteristics are given in Table 1-1, and it is shown in cross section in Figure 2-4. It was ruled holographically on an optical master and then replicated onto the stainless steel blank. For Astro-2, the grating has been coated with silicon carbide and is about 80% more efficient than the osmium-coated grating used on Astro-1.

Calibration Lamp

The ultraviolet calibration lamp is a quartz mercury discharge tube and is mounted on the opposite side of the spectrometer from the detector. It is indicated as the ``Reference lamp'' in Figure 2-4. From this location, two of the spectral lines produced by the lamp fall on the detector face. A wide slit placed over the lamp provides lines that are about 80 pixels wide, with a weak line located near pixel 1660 and a very weak secondary line near pixel 1490. These UV emissions are used to test the operation of the detector and spectrometer subsystems and provide a means of tracking any degradation of the sensitivity throughout the instrument integration. They do *not* provide a wavelength calibration, nor do they yield a photometric calibration of the instrument.

6/23/1999

Vacuum Pumps

The detector is not sealed with a window and its photocathode material is sensitive to degradation in air, so it must be maintained in a vacuum at all times throughout the preparations for flight. Two redundant vacuum ion pumps are provided to maintain a vacuum within the spectrometer, and a valved pump-out port allows the use of an external pump during much of the ground operations. The two small internal pumps are 2 liter sec^{-1} Varian ``VacIon'' pumps, which are powered by individual high voltage power supplies mounted on the spider arms. Several different power sources are available for these pumps. For orbital operations, the power is supplied by either the Spacelab Experiment Power Distribution system or by the Shuttle's payload cabin power. For ground operations, the power is also supplied by a number of external power supplies through various connectors including finally the T-0 umbilical when Astro is installed in the Shuttle.

Detector

Figure 2-5: A schematic drawing of the intensified photodiode array detector.

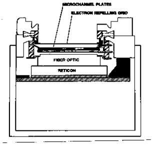

The detector is an intensified photodiode array and is described in detail by Long et al. (1985). The image intensifier portion of the detector consists of two 25 mm 80:1, 10 μm pore microchannel plates (MCP's) and an aluminum-overcoated P 20 phosphor deposited on a 6 μm pore fiber optic, all mounted into a modified Varian Conflat flange. The photocathode material is cesium iodide (CsI) deposited, in a thin layer, directly to the front surface of the top MCP. Mounted against the back of the intensifier fiber optic is a 1024 channel Reticon photodiode array. The individual photodiodes are $25\ \mu\mathrm{m} \times 2.5\ \mathrm{mm}$. Individual photon events produce a detectable signal in about 12 photodiodes. The array is scanned and digitized in 1 msec by the Reticon control electronics, which is mounted close to the detector on one of the spider arms. The Spectrometer Processor (SP) then centroids these events to an accuracy of 1/2 diode and provides a 2048 pixel histogram of the location of each photon on the detector. This gives a wavelength accuracy of $\sim$ 0.5 Å. In high time-resolution mode the SP also outputs a list of events with their locations and a time tag accurate to ~ 1 msec. Characteristics of the detector system are listed in Table 1-1 and a schematic is shown in Figure 2-5.

6/23/1999

Acquisition TV Camera

The TV camera, mounted on the one of the spider arms, is used to provide accurate pointing information for the telescope. The camera was built by Videospection (formerly EDO-Western). A 9 x 12 arcmin field surrounding the source is reflected from the aperture disk and reimaged by a transfer lens onto the face of the TV camera. The camera incorporates an RCA 4804 Silicon Integrating Target (SIT) vidicon tube and a number of neutral density filters to permit observation of targets as faint as V=17 or as bright as V=-4. The TV image is digitized in the DEP, using a 4 bit A/D converter, and stored in a video RAM. The image update rate depends on a number of factors (such as the amount of processing time required to calculate centroids, or the integration time needed for faint targets, etc.), but typically varies from 2 to 16 seconds. The digitized image is displayed on the Shuttle's Closed Circuit TV (CCTV) system and used by the crew to center the source in the spectrometer aperture at the start of an observation. Centering is accomplished by issuing commands to the IPS with a manual pointing controller (joy stick) or from an error signal generated by the DEP. After an observation is started, the TV image is used to provide tracking information from selected guide stars in the field.

OPERATIONS

6/23/1999

Overview

Since HUT remains in the shuttle bay for the extent of a mission and relies on the shuttle for power, telemetry, and pointing control, it was designed to be operated much like a modern ground-based telescope rather than a free-flying spacecraft. Just as the telescope operator and the astronomer work together to point a telescope on the ground and operate the attached instrument through computer control, the shuttle crew, the mission specialist (MS), and the payload specialist (PS) maneuver the shuttle, control the instrument pointing system (IPS), and operate HUT with a set of computer terminals aboard the shuttle. There are several different methods of target acquisition and pointing control for the Astro telescopes, which will be described in more detail below, but the basic observing sequence for a target is similar in all cases. After a shuttle maneuver to orient the observatory and an IPS slew to the target, the MS and the PS use the video display from the HUT acquisition TV camera to identify the target and center it in the HUT aperture using manual commands to control the IPS pointing direction. The IPS then normally tracks the guide stars identified in its three star trackers to stabilize the pointing. The instruments are set up in the appropriate configuration for the current target, and the observation is commanded to begin.

While the shuttle crew has primary responsibility for shuttle and instrument control, many of these operations can also be commanded from the Payload Operations Control Center (POCC) at MSFC, and ground control of the instruments was the mode of operation used for the Astro-1 mission after the failure of both data display units (DDU's, the computer terminals) aboard the shuttle. This experience showed that ground commanding actually has many advantages for specific aspects of Astro operations, and operational procedures for Astro-2 are being developed that will combine the best features of crew and ground control.

Ground operations in the POCC also play a significant role in maximizing the scientific return during the Astro missions. More than 80% of the science data from HUT is available in real time in the POCC. These data are analyzed nearly in real time to optimize the configuration of HUT (*e.g.*, optical alignment, focusing, detector performance, etc.) and to evaluate the results of observations. The POCC team replans the science timeline based on these real time results to make sure that the highest priority observations are successfully completed before the end of the mission.

The following sections give more details on specific aspects of mission operations as they relate to HUT.

6/23/1999

HUT Operations

Nearly all HUT operations are controlled through the Dedicated Experiment Processor (DEP), except for special operations performed off-line during experiment integration. Detailed expositions of the following sections can be found in the HUT Dedicated Experiment Processor Software Requirements Document, Rev. E, April 1990.

6/23/1999

The Command Interface

Commands generated by the crew or telemetered to the shuttle from the POCC operate HUT through the Spacelab Experiment Computer (EC) and its Experiment Computer Operating System (ECOS) and Experiment Computer Applications Software (ECAS). The EC communicates with HUT through the Remote Acquisition Unit (RAU). The RAU directly commands and monitors the essential instrument survival subsystems (such as main power, heater power, the Vac-Ion pumps, and DEP power and initialization). Once the DEP is operational, it processes commands and monitors HUT's basic subsystems and science subsystems. The HUT science subsystems provide data to the SP for analysis. The SP feeds the processed data to the DEP for formatting in the High Rate Multiplexer (HRM) data stream for transmission to the ground.

HUT commands are issued from five display pages which can be brought up on the PS's DDU. (Copies of these display pages may also be viewed in the POCC.) These displays provide a visual reminder of the discrete commands required for each function, display associated status data, and provide visual and audio alerts when parameters exceed pre-specified warning limits or when errors occur. The display pages are

- HUT Activation
- HUT Operations
- HUT Spectrometer
- HUT Doors and Camera
- HUT Mirrors and Heater

and their basic format is shown in Figures 3-1 to 3-5. The HAC display is generated by an ECAS task using data directly from the RAU, while the others are DEP allocated displays which require the DEP to be active for use. As one might gather from the names, the HAC page is used to perform the most basic functions necessary for powering HUT up and down. Most observational procedures are controlled by high level sets of commands issued from the HOP page. HSP, HDC, and HMH provide control of individual subsystems on HUT.

Figure 3-1: Display: HAC HUT Activation.

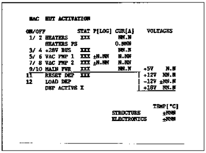

Figure 3-2: Display: HOP HUT Operations.

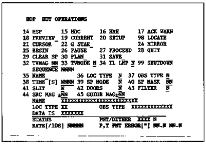

Figure 3-3: Display: HSP HUT Spectrometer.

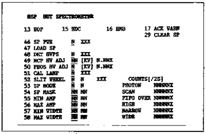

```
HSP  HUT SPECTROMETER

13 HOP      15 HDC        16 HMH       17 ACK WARN
                                       29 CLEAR SP
46 SP PWR       N  XXX
47 LOAD SP
48 DET HVPS     N  XXX
49 MCP HV ADJ   NN [KV] N.NNX
50 PHOS HV ADJ  N  [KV] N.NNX
51 CAL LAMP     N  XXX
52 SLIT WHEEL   N  N    XXX      COUNTS[/2S]
53 SP MODE      N  N            PHOTON    NNNNNX
54 SP MASK      NN NN           SCAN      NNNNNX
55 MIN AMP      NN NN           FIFO OVER NNNNNX
56 MAX AMP      NN NN           HIGH      NNNNNX
57 MIN WIDTH    NN NN           NARROW    NNNNNX
58 MAX WIDTH    NN NN           WIDE      NNNNNX
```

Figure 3-4: Display: HDC HUT doors and camera.

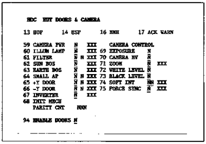

```
HDC  HUT DOORS & CAMERA

13 HOP      14 HSP       16 HMH      17 ACK WARN

59 CAMERA PWR   N    XXX    CAMERA CONTROL
60 ILLUM LAMP   N    XXX 69 EXPOSURE    N
61 FILTER       N N  XXX 70 CAMERA HV   N
62 SUN BOS      N    XXX 71 ZOOM        N   XXX
63 EARTH BOS    N    XXX 72 WHITE LEVEL N
64 SMALL AP     N N  XXX 73 BLACK LEVEL N
65 +Y DOOR      N N  XXX 74 SOFT INT    NN  XXX
66 -Y DOOR      N N  XXX 75 FORCE SYNC  N   XXX
67 INVERTER     N    XXX
68 INIT MECH
   PARITY CNT    NNN

94 ENABLE DOORS N
```

Figure 3-5: Display: HMH HUT mirror and heater.

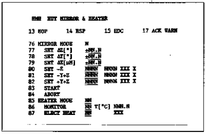

```
HMH  HUT MIRROR & HEATER

13 HOP      14 HSP       15 HDC      17 ACK WARN

76 MIRROR MODE     N
77   SET ΔZ["]     ±NN.N
78   SET ΔY["]     ±NN.N
79   SET ΔX[μM]    ±NN.N
80   SET -Z        NNNN  NNNN XXX X
81   SET -Y+Z      NNNN  NNNN XXX X
82   SET +Y+Z      NNNN  NNNN XXX X
83   START
84   ABORT
85 HEATER MODE     NN
86   MONITOR       NN T["C] NNN.N
87   ELECT HEAT    NN       XXX
```

6/23/1999

Downlink Data Formats

While a limited amount of HUT housekeeping information is downlinked in the data stream generated by the Spacelab EC, the full set of HUT engineering parameters and science data require a much higher bit rate. The DEP formats a variety of telemetry frames for transmission through one 97,656 bit per second HRM channel. There are 8 basic telemetry frame formats as summarized in Table 3-1.

Table 3-1: HUT HRM Data Formats

Frame type	Mnemonic	Description
1	hg	Histogram data
2	ss	Single scan data
3	cu	Cumulative unprocessed data
4	ht	High time resolution data
5	ph	Periodic histogram data
6	so	Status only data
7	iv	Integrated video data
8-15	vd	TV camera video data

The first six of these modes have a direct correspondence to the operational mode of the SP. During typical science observations, spectrograph data are transmitted either in histogram mode, with a 2048 pixel cumulative spectrum downlinked every 2 s, or in high time resolution mode. In high time resolution mode, individual events are tagged by location (1 to 2048) and arrival time to a precision of $\sim$1 ms. These frames are transmitted every 2 s. Every 60 s in high time resolution mode a cumulative histogram is transmitted as a periodic histogram frame. This ensures that no data useful for producing a time-averaged spectrum are lost even if data dropouts cause the loss of individual ht frames, or high count rates prevent all events from being transmitted. (Sources must have total count rates, including airglow, less than ~ 500 cts s^{-1} to prevent the buffers from overflowing in high time resolution mode.)

Single-scan and cumulative unprocessed data are used for detector diagnostics such as forming pulse-height distributions. Each of the science frame types (1-5) has an engineering status header. This status section is transmitted as a status-only frame every 2 s whenever the SP is hibernating (a self-test state used during South Atlantic Anomaly passages) or turned off, or whenever the detector is off.

Video frames from the HUT TV camera are transmitted as an eighth of a full frame every 2 s. Thus it takes 16 s to transmit one full video frame. These frames have intensities digitized to 4 bits, so they serve to identify stars, but they do not make spectacular astronomical images.

A higher dynamic range can be achieved by requesting a software video integrated picture. In this mode the DEP integrates a 16 bit image over a 43 × 53 pixel region around the center of the TV field of view for the requested integration time. This can be useful for identifying extremely faint targets.

DEP Operational Modes

The display on the HOP page can be in one of three operational contexts. The ``Current'' context is the normal display, and it reflects the actual state of the HUT configuration. The ``Plan'' context is used to change the instrument parameters located in one of the five sequence files stored in the DEP memory, either by starting from scratch, or by using data from a specified sequence load. The ``Preview'' context displays the configuration to be used for the next observation and loads it into the buffer used by the DEP when the SETUP command is given. The instrument configuration to be used can be changed in the ``Preview'' buffer before the SETUP command is given.

The DEP itself can be in one of eight operational states: Reset, Load, Ready, Setup, Locate, Observe, Pause, or Slew. The DEP enters Reset mode upon power up or when given a hardware reset. After completion of the reset sequence, the DEP is ready to accept the initialization load and program data. Loading the DEP requires $\sim$ 7 minutes. After a successful load the DEP enters the Ready state.

The SETUP command to configure HUT for an observation places the DEP in the Setup mode. The observation sequence residing in the preview buffer is then used to configure HUT for the next observation. At any time in Setup mode, the configuration can be changed by sending appropriate commands in the Current context.

Once HUT has reached the requested configuration (this can take a few minutes if several mechanism motions are required), the DEP proceeds from Setup mode to Locate mode. The DEP will then locate the target using the method specified in the sequence load. Table 3-2 summarizes the locate modes, the typical target types they are used for, and the method used. The DEP configures the HUT TV camera appropriately for the chosen locate mode. For Source and Manual locate, the TV camera magnitude is set to the target magnitude. For Guide Star and None locate, the TV camera is adjusted for the mean guide star magnitude.

Table 3-2: HUT Locate Modes

Mode	Target Type	Locate Method
Source	Visible point source	Use the target itself
Manual	Complex field	Use the cursor location
Guide Star	Invisible or extended sources	Use guide star positions
None	Moving targets, background measurements	None

After the PS is satisfied that the target is properly centered in the HUT aperture, the BEGIN command places the DEP in Observe mode. HUT can be reconfigured during an observation by issuing appropriate commands while in the Current context, or the next observation can be configured by editing a sequence in the Preview contexts. The DEP exits Observe mode either upon receiving a PAUSE, QUIT, or SETUP command, or if the planned observation time is completed. The observation time buffer is decremented starting from the BEGIN command, and it does not stop for any reason.

When the DEP enters Observe mode, it moves the primary observing slit into place if not already there, sets the TV camera parameters for the mean guide star magnitude, and locks on to the selected guide stars *at their locations when the BEGIN command was issued.* All subsequent pointing errors are referenced to this initial location of the guide stars. Complex observations can be pre-programmed into an observing sequence. A ``dither'' will change the selected telemetry mode, the observing slit, and any mask applied to the spectrum by the SP after a selected time interval. (The SP can be directed to ignore events in certain regions of the detector such as around geocoronal Ly$\alpha$ by selecting a particular ``mask''.) When the time specified for the Secondary observation interval is completed, the DEP will repeat the Primary observation interval, and so on until the observation is complete.

Up to 3 Offset pointing positions can be specified in the sequence definition, each with a requested observing time. The DEP moves the HUT mirror to achieve the specified pointing offsets. A regular pattern of offset pointings can be accommodated by using a Raster observation. The sequence load specifies the step size ΔY and ΔZ in the HUT coordinate system, the number of Y and Z steps, and the integration time per dwell point in the pattern.

The PAUSE command can be used to suspend a Dither, Offset, or Raster observation. Data continues to accumulate in the current configuration in the Pause mode. If a Pause is suspended with a PROCEED command, Observe mode resumes. One may also exit Pause mode by commanding a QUIT, BEGIN, or SETUP.

When the planned observation time runs out or a QUIT command is given, the DEP enters SLEW mode. The DEP uses the special sequence 0 stored in memory to configure the instrument for SLEW mode. The maximum attenuating filter is placed in front of the TV camera to protect it against bright objects during a SLEW. If the detector is on, background can be accumulated either as dark count if the slit is closed, or airglow data can be accumulated as the shuttle maneuvers to acquire the next target.

Target Acquisition and Pointing Control

6/23/1999

Automated Acquisitions with the IPS

The IPS was designed to provide all necessary target acquisition and pointing control for the Astro telescopes, supplemented by the HUT acquisition TV camera and the ASTROS Star Tracker (AST) mounted on UIT. Three fixed-head star trackers (FHST's) comprise the optical sensor package (OSP) of the IPS, one bore-sighted with the telescopes, and the other two skewed at 12° angles to either side. Gyros provide information on short-term motions and preserve knowledge of the pointing direction during slews and other intervals when the OSP is not tracking stars. Once the gyro drift rates and the tracker orientations and sensitivities are calibrated in orbit and the IPS is pointed at a star with known coordinates, it knows in principle where it is pointed at all times. Knowledge of the pointing direction can be updated at every target acquisition.

After OSP calibration (OSPCAL), the IPS pointing direction is initialized with a procedure called Identification Initial, or ``IDIN''. This requires the bore-sight tracker to be pointed at a bright, isolated star. The subsequent stellar acquisitions used for routine observations use a procedure called Identification Operational, or ``IDOP''. IDOP's use the brightness, coordinate location, and separation angle of pre-selected guide stars identified in two or more of the star trackers to determine the IPS pointing direction. After a successful IDOP, the IPS adjusts the pointing direction to match the desired coordinates and enters optical hold by tracking the identified guide stars. Successful IDOP's should place the desired target within several arc seconds of the center of the HUT field of view. In optical hold, the IPS jitter about the current pointing direction is typically less than $1''$ rms in radius.

Once the IPS has completed a successful IDOP, the PS or MS identifies the target to be observed and centers it in the HUT aperture, using either a bias command if HUT has successfully identified the target or the manual pointing controller if it has not. The IPS knowledge of the pointing direction can then updated, and the observation can proceed. Since the IPS is already in optical hold, it provides stable pointing control for the remainder of the observation.

Manual Target Acquisition

Due to problems in calibrating the sensitivity and relative orientations of the star trackers, IDOP's were rarely successful on Astro-1. Most target acquisitions were done in a manual mode that used the JPL-provided ASTROS Star Tracker (AST) mounted on UIT. The AST is a CCD-based tracker with a large ($2.5^{\circ} \times 2.2^{\circ}$) field of view. The AST identifies the three brightest stars in its field and displays the magnitude and coordinates of these stars to the crew. Using the displayed coordinates and a finding chart generated specifically for each target, The PS or MS uses the manual pointing controller to orient the IPS and place the target in the field of view of the HUT TV camera.

Once the target has been acquired, the IPS knowledge of the pointing direction can be updated, but the IPS is not in optical hold after a manual target acquisition. Pointing stability at this point is provided only by the IPS gyros, and tracking for the rest of the observation must be provided by one of the following methods.

Manual Pointing Control

This is the method used for most observations on Astro-1. Here the astronauts use the guide stars identified in the HUT TV camera field of view to keep the target centered in the HUT aperture using the manual pointing controller, just as a ground-based observer would use a button-box or joy stick to guide the telescope during an observation. When guide stars were available, the crew on Astro-1 did an excellent job of maintaining pointing stability. For most observations the rms pointing jitter was typically <2" in radius, only a factor of ~ 2 worse than the IPS in optical hold. Several observations, particularly those of bright stars, had no visible guide stars, however, and the only way to guide was a combination of looking for light leaking from the edge of the HUT aperture and guessing pointing corrections that would compensate for the gyro drift rates.

Lock on Target

For Astro-1 the only method of placing the IPS in optical hold was to achieve a successful IDOP. For Astro-2 this software limitation has been circumvented by designing a new tracking mode known as lock-on-target (LOT). In this mode each of the trackers is commanded to search its field and to acquire and lock onto the first star it finds without using any position or brightness criteria. The crew has identified the field using the HUT TV camera, so *they* know where the IPS is pointed, even if it doesn't. This permits the crew to then track targets with the IPS in optical hold no matter how the target acquisition was performed in the first place.

Sensor Substitution

A final option for pointing control after target acquisition is to substitute tracking information from the AST to the IPS control loop instead of the data from the OSP. This mode was designed for Astro-1 in case the IPS were to malfunction (as it did). Unfortunately, various problems, including poor knowledge of the alignment, errors in the coordinate systems used, and timing errors in the control loop also prevented sensor substitution from working. All these problems have been resolved, and this mode should provide another viable pointing control method for Astro-2.

POCC Operations

6/23/1999

POCC Capabilities

The Payload Operations Control Center (POCC) at Marshall Space Flight Center (MSFC) in Huntsville, Alabama, is the ground control center for Spacelab missions. Real-time data from the experiments aboard the shuttle are relayed via the Tracking and Data Relay Satellite (TDRS) and a domestic communications satellite to the POCC. The POCC also receives live audio and video from the shuttle, and it can uplink voice and commands to the shuttle through mission control at Johnson Spaceflight Center (JSC) in Houston. Within the POCC these data and communication lines are distributed over an internal network to individual experimenters' stations in the facility. Each station has access to the POCC internal communications loops, video displays, displays of shuttle ground tracks and times of AOS/LOS (acquisition and loss of signal from the shuttle), and terminals connected to the POCC Peripheral Processor system and the POCC VAX cluster. All positions in the HUT area of the POCC also have terminal connections to the HUT ground support equipment (GSE) computers which process the HUT HRM data.

The POCC Peripheral Processor system is a cluster of MicroVAX 2's which access the POCC database. The PP's can create customized displays of data in the database stored from the telemetry transmitted by the Spacelab EC, or uplink commands and data to the shuttle.

The POCC VAX cluster supports software comprising the Operations Management Information System (OMIS), an electronic database/bulletin board/memo system. OMIS is used to request, manage and track most requests that affect mission operations during the flight. For example, all changes to the science timeline are initiated by submitting electronic Replanning Requests (RR's) at least 24 hours in advance of the desired change. Changes to operations on shorter timescales are managed by Operation Change Requests, or OCR's. The system is cumbersome, slow, and frustrating to use, but it provides a good record, and it sure beats paper.

POCC Positions and Schedule

The HUT team in the POCC is divided into two 12-hour shifts of 11 people each who cover all essential areas of HUT ground operations. These positions are listed in Table 3-3.

Table 3-3: HUT POCC Positions

Position	Responsibility
PI/Rep	Interface with mission management
	Make strategic scientific and technical decisions
A/G Lead	Manage instrument operations
	Sole representative for crew communications
Engineer #1	Assist in instrument operations; evaluate instrument performance
Engineer #2	Assist in instrument operations; evaluate instrument performance
DEP S/W	Assist in instrument operations and data uplinks
	Evaluate DEP performance
Data Evaluator	Evaluate science and calibration data
	Track science objectives
Data Flow Manager	Monitor reception of HUT HRM data and archive to tape
	Monitor GSE performance
Replanner #1	Monitor mission timeline changes
	Re-plan science observations to achieve team science goals
Replanner #2	Monitor mission timeline changes
	Re-plan science observations to achieve team science goals
PATSI	Problem Analyst and Troubleshooting Investigator
	Assist in analyzing instrument performance,
	science and calibration data, planning software,
	GSE performance, and preparing data uplinks
Team Administrator	Manage paper flow; team interface to the real world

The schedule in the POCC revolves around the crew schedule aboard the shuttle. Each shift begins with a meeting of the Science Operations Planning Group (SOPG), and the meeting time coincides with crew handovers. The SOPG is chaired by the Mission Scientist or Deputy Mission Scientist and is attended by each instrument PI or their representative, and other supporting personnel as needed. The SOPG monitors the scientific goals of the mission and instrument performance, and it is the decision-making body for all changes to the mission timeline or operations which affect science operations. The SOPG generally makes decisions about operational changes that will affect the shift that begins with the *next* SOPG, i.e., 12-24 hours later. (Final authority for implementing many changes rests with mission control at JSC if decisions affect the orbiter or crew safety.)

The times of other key operations in the POCC are referenced to the beginning of the SOPG meeting. Each HUT position is manned for 12 hours with an additional hour of overlap time for one shift to hand over operations to the next shift. During a handover all personnel jointly fill out a shift report with their counterparts which summarizes the activities of the previous twelve hours. This serves to brief the oncoming shift and prepare them to smoothly assume the tasks of the previous shift. Handovers are staggered in time to keep the POCC area from getting too crowded. The PI/Rep, the A/G Lead, and Engineer #1 arrive 30 m prior to the SOPG; their handovers are not completed until *after* the SOPG is finished. The DEP S/W, Data Flow, and Data Evaluator positions arrive just after the beginning of the SOPG and are encouraged to depart before it ends. The remaining positions arrive 30 m after the start of the SOPG, and their handovers are completed after it is over.

CALIBRATION

Transforming the raw HUT data to flux and wavelength calibrated spectra requires several steps. Important transformations include corrections for wavelength shifts induced by image motion, pulse persistence resulting from the phosphor decay time, dark-count subtraction, dead-time corrections, scattered light subtraction, subtraction of second-order emission, flat-field corrections, and multiplication by the inverse sensitivity curve. Additional corrections to the overall flux scale to correct for light lost due to image motion are also made. To take advantage of the statistical properties of the photon-counting HUT detector, we compute and propagate an error array for each step in the data reduction process. We describe each of the corrections to the HUT data in more detail in the following sections.

6/23/1999

Wavelength Calibration and Image Motion Corrections

The HUT wavelength scale is well described by a simple linear relation between pixel number and wavelength. For pixel numbers running from 1 to 2048, the wavelength is given by $\lambda = 827.36 + 0.51336(n-1)$.This was verified to be stable to within ± 1 Å in flight during Astro-1 using airglow lines.

The HUT observing apertures are quite large, and typical image motions can induce shifts in the zero-point of the wavelength scale for point sources. Offsets of 1$''$ in the dispersion direction correspond to wavelength shifts of 0.33 Å. Nominal performance of the IPS during optical hold is 1$''$ rms radius, with excursions of many arcsec during thruster firings for station keeping. Nearly *all* Astro-1 observations, however, were done under manual pointing control. The payload specialists were able to nearly match the expected performance of the IPS when suitable guide stars were visible in the field of the HUT acquisition TV camera, but most observations of bright stars had no visible guide stars, and pointing errors in these cases typically span the entire width of the aperture.

Timescales for the jitter in optical hold or under manual pointing control is of order several seconds. Pointing information from the Image Motion Compensation System (IMCS) is available at a 50 Hz rate, and HUT data acquired in high time-resolution mode can take full advantage of this information. In practice, we have found that corrections on the 2 second timescale of the histogram data mode is adequate to compensate for nearly all the image motion. Thermal drifts between the ASTROS Star Tracker (AST) and the HUT boresight introduces an offset of the IMC reference direction of several arcseconds on timescales of tens of minutes.

To correct for the wavelength shifts induced by image motion we first correct the IMC reference signal for the slow thermal drift by fitting a low order polynomial to the relative change in the AST pointing direction. Next, we compute the mean offset over the 2 second integration interval for a HUT data frame from the IMCS data. This is translated into a wavelength offset, and the data frame is shifted by the corresponding integer number of pixels before accumulation into the buffer for the observation.

These wavelength corrections in effect remove most of the spectral smearing induced by the image motion and permit one to recover the full instrumental spectral resolution of~ 3 Å for a point source. Airglow lines, whose emission fills the entire aperture, are correspondingly smeared into even broader features, however. To permit subtraction of the smeared airglow lines, a Lyα template profile is shifted in the same manner as the observed spectrum. This profile can then be used to model and subtract airglow emissions from the spectrum.

Wavelength offsets are still possible in the corrected data if the observation was started with the target mis-centered in the aperture. Corrections for such mis-centering must be determined off-line by examining the positions of guide stars (if available) relative to the slit center in the acquisition TV images.

6/23/1999

Pulse Persistence

Light pulses in the phosphor readout of the HUT detector have a decay time of 0.20 ms. Since the Reticon diode array is scanned once every 1.024 ms, a small fraction of pulses have persistence bright enough to be flagged as genuine events on the subsequent scan of the diode array. These double-counted events can be easily identified in high time-resolution mode. Measurement of the pulse persistence during observations of high count-rate targets on Astro-1 shows that statistically 92.6% of the recorded counts correspond to true incident photons. In the standard reduction of HUT data, we have chosen to fold this simple multiplicative correction to the count rates into the inverse sensitivity curve.

Since the HUT detector is photon counting, errors in the detected count rate follow a Poisson distribution. To assign errors to the individual pixels in a spectrum we use the square root of the detected number of photons. It is in this error bar calculation that the pulse persistence correction must be explicitly incorporated since the actual number of photons is only 92.6% of the number of recorded counts. Thus, the assigned error for a pixel containing N counts is not $\sqrt{N}$, but $\sqrt{N/0.926}$.

Dead Time

Dead-time corrections are important (i.e., are greater than 1%) only for line emission above 30 count s^{-1} integrated over the line, or > 4 count $pixel^{-1}s^{-1}$ at the peak for a line of 3 Å full-width at half-maximum (FWHM), or > 3 count $pixel^{-1}s^{-1}$ at the peak of a 6 Å FWHM line. Continuum emission limits are lower, with corrections important only at rates exceeding 1 count $pixel^{-1}s^{-1}$. Since few HUT targets exceed these rates and since the Monte-Carlo detector model is computationally expensive, dead-time corrections are not routinely calculated for all HUT spectra in the reduction process. When appropriate, these calculations must be done off-line separately for each observation.

6/23/1999

Dark Count

The dark count in the HUT detector system is principally due to charged particle events. These particle-induced events account for about 65% to 95% of the detector background during orbital night. The balance of the background is due to scattered light from airglow emission, and its level depends upon the aperture selected for the observation as well as the position of the shuttle in its orbit and the pointing direction. Measurements made during three long observations on Astro-1 with the spectrograph aperture closed detected dark count rates ranging from 3.55 times 10^{-4} 4.70 times 10^{-4} count $pixel^{-1}$ s^{-1} spread uniformly across the spectrum. The mean dark rate was $\$3.94 \times 10^{-4}$ count $pixel^{-1}$ s^{-1}.Similar count rates are anticipated for Astro-2.

6/23/1999

Scattered Light

Figure 4-1: HUT Astro-1 Lyman-α scattering profile for the 18$''$ circular aperture.

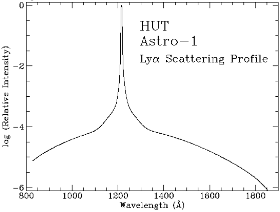

Scattered light from geocoronal Lyα accounts for the remainder of the background in a spectrum, and for the largest apertures it can dominate over the dark count during orbital daylight. The holographic grating used in the HUT spectrograph has excellent scattered light characteristics with no ghosts. Far from the line center, scattered light is roughly uniform across the spectrum at a level of $\sim 10^{-5}$ $Å^{-1}$ times the integrated intensity of the incident emission line. This is approximately a factor of ten lower than for comparable ruled gratings. Scattering profiles for geocoronal Lyα were measured through each aperture used on Astro-1 during orbital night in observations of blank fields. The fitted profile for the 18$''$ circular aperture used on Astro-1 is shown in Figure 4-1. The profile is expected to be similar in the 20$''$ circular aperture on Astro-2.

In the pipeline processing of HUT data only the roughly uniform contribution to the scattered light is subtracted from each spectrum. This is computed from the residual count rate after dark-count subtraction in an airglow-free region spanning 845-885 Å below the 912 Å cutoff due to neutral hydrogen in the local interstellar medium. For faint sources the wings of the Lyα scattering profile can be significant. Removing this emission accurately requires fitting the line profile template to the raw data, and this is best done by the user interactively in off-line processing.

Second-order Light

While the aluminum filter in aperture 3 blocks long-wavelength radiation for a clean view of the second-order spectrum, the only filter available to HUT for blocking short-wavelength light is the natural absorption below 912 Å due to the Lyman edge of neutral hydrogen in the local ISM. Since the red end of the HUT spectrum extends to 1860 Å diffracted light in second order appears over the 1824-1860 Å interval. This is removed by using the observed first order spectrum over the 912-930 Å interval, and scaling it by the measured ratio of the second order to first order efficiency of the grating. This ratio was measured to be 0.226 for Astro-1.

Flat Fields

Figure 4-2: Flat field correction for Astro-1 observations made through the 50 cm^2 small aperture door. A modification for Astro-2 is expected to eliminate the fixed pattern seen here.

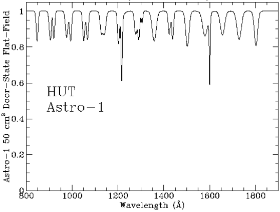

Figure 4-3: Observed (raw) count spectrum for a 366 s observation of the DA white dwarf G191-B2B. Pixels, 0.51 Å wide, have been converted to a wavelength scale. The Lyman-series lines are seen clearly. Lyman-α is partially filled in by geocoronal emission. The Lyman edge produced by interstellar hydrogen is also evident. The apparent absorption feature at 1600 Å, marked with an asterisk, is an artifact, due to a small dead spot on the detector.

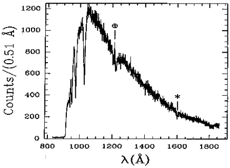

Small-scale, pixel-to-pixel variations in the sensitivity of the HUT detector have three principal sources. First, a negatively charged grid is placed in front of the photocathode to enhance the capture efficiency of ejected photo-electrons. This grid has a transmission of 95%, and it is far enough from the focal plane that the pattern is highly defocussed in the $f/2$ beam of HUT. When bright targets are observed through the small aperture doors, however, the much slower effective focal ratios cause the grid to cast distinct shadows on the detector. For Astro-1 these shadow patterns were measured in the Synchrotron Ultraviolet Radiation Facility (SURF) at the National Institute of Standards and Technology (NIST) in Gaithersburg, MD. The resulting flat field correction for the 50 cm^2 small aperture door is shown in Figure 4-2. For Astro-2 the repelling grid in front of the photocathode has been modified so that no wires cross the region illuminated by the focussed spectrum. Thus these shadow patterns should be eliminated.

Figure 4-4: (a) A comparison of the postflight laboratory effective area curve against the in-flight effective area curve derived from the G191-B2B model atmosphere. The individual postflight data points are indicated as well. (b) The ratio of the G191-B2B-based effective area curve to the postflight laboratory effective area curve.

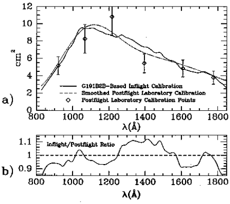

The second source of small-scale sensitivity variations is defects or non-uniformities in the photocathode or the microchannel plate. Only one such spot was identified on the HUT detector for Astro-1, located at 1600 Å, and it is only noticeable in spectra obtained in half-aperture or small aperture door observations. This feature can be seen in the spectrum of G191-B2B as noted on Figure 4-3, and it is also apparent in Figure 4-2.

The third source of sensitivity variations is in the pair of amplifiers used in reading the Reticon diode array. One amplifier serves the odd numbered diodes, and another the even ones. These are balanced so that the resulting signals differ by less than 1%. The residual imbalance produces an odd/even pattern that is noticeable at the $\pm$0.5% level in the highest S/N spectra. The odd/even pattern does not appear to be stable, and so no correction is currently applied to the HUT data in routine processing.

6/23/1999

Flux Calibration

The HUT flux calibration for Astro-1 is based upon pre-flight and post-flight laboratory calibrations directly traceable to NIST standards, and upon in-flight observations of the hot white dwarfs G191-B2B and HZ 43. This combination of calibrations and cross-checks makes HUT the best calibrated instrument for far-ultraviolet astronomy yet flown.

The effective area curve for HUT is directly based on a white dwarf model atmosphere for G191-B2B as described by Davidsen et al. (1992) and Kimble et al. (1993). The raw data from the 366 s observation of G191-B2B were corrected for pulse persistence, dark counts, scattered light, dead time, and second-order and third-order light as described in the previous sections. The model atmosphere calculation is described by Holberg et al. (1991), and it assumes T_{eff}=59250 K, log g = 7.5, and V = 11.78. The model is multiplied by the transmission function of the local ISM for $N_H = 1.7 \times 10^{18}$ cm^{-2} and b = 10 km s^{-1}, and smoothed to the HUT resolution. Division of this model into the corrected count rate spectrum yields the effective area curve for the half-aperture door state used for the observation. The correction to the full aperture curve shown in Figure 4-4 (a) was made by multiplying by the ratio of full-aperture to half-aperture sensitivity, derived separately from observations of several stars that were observed in both half-aperture and full-aperture modes. Structure on scales less than 25 Å in the curve was removed by smoothing the raw curve with a Gaussian of dispersion 10 Å. Before smoothing, 5 Å regions surrounding the cores of Lyβ, Lyγ ,Lyδ, and the 1600 Å feature were replaced by linear interpolation of the surrounding pixels. A 15 Å region centered on Lyα was similarly replaced. To obtain the effective-area curve shortward of 920 Å, where the observed flux of G191-B2B goes to zero, we have used pre-flight calibration points at 835, 879, and 920 Å. A linear least-squares fit was made to these points and scaled down (by 27%) to join smoothly onto the in-flight calibration curve at 920 Å.

A full end-to-end laboratory calibration of the assembled instrument was not possible within the scope of the HUT program. The in-flight measurements run $\sim$20%-30% below the pre-flight values, probably due to aging of the photocathode. Our measurements of the on-board calibration lamp over time indicate a decline in efficiency of 24%. We also measured a similar decline in sensitivity (in both magnitude and spectral shape) over several years in the original HUT spectrograph, which was replaced after the *Challenger* accident.

The post-flight laboratory calibration of the HUT spectrograph was performed in January 1992 at seven wavelengths distributed across our spectral range. These effective areas are also shown in Figure 4-4 (a) as discrete points. The ratio of the post-flight to pre-flight laboratory efficiencies is well fitted by a smooth curve varying from $\sim$0.85 to $\sim$0.65 across our first-order wavelength range. This degradation is consistent with our previous experience as described above. The pre-flight effective area data for the full instrument are also well fitted by a smooth curve. The product of these two curves yields another smoothly varying function that represents our best estimate for the in-flight efficiency of HUT, based purely on our laboratory calibration, and traceable to standards maintained by the National Institute of Standards and Technology. This laboratory calibration curve matches the G191-B2B-based in-flight calibration curve *almost exactly*, as shown in Figure 4-4 (a).

The ratio of the laboratory calibration curve to the in-flight curve [Figure 4-4 (b)] has a mean value of 1.003 with an rms deviation of 6.6%, and maximum deviations of +12% and -8%. We emphasize that no re-scaling has been done to achieve this impressive agreement. These results provide powerful confirmation that (1) there are no significant systematic errors in the HUT flux calibration, and (2) the G191-B2B model atmosphere calculations provide an excellent flux standard for the far ultraviolet. We believe our observation of G191-B2B constitutes the best existing absolute UV flux measurement (i.e., directly traceable to laboratory standards) of a star that is suitable as a primary flux standard throughout the vacuum ultraviolet region of the spectrum, all the way to the Lyman limit.

Comparison of the Bergeron model to an independent model calculation for the same $T_{\rm eff}$ and $\log g$,kindly provided by D. Koester, shows differences at the level of <5%. Comparison of the data and the models gives some idea of the internal consistency of the calibration, though, of course, it yields no information on possible systematic errors in absolute flux calibration. These could arise, for example, from deviations of the real white dwarf atmosphere from the model atmosphere or from unknown errors in our data reduction procedure.

Uncertainties in the G191-B2B temperature (derived from Balmer line profiles) translate to less than 5% changes in the model-predicted far-UV flux down to within a few Å of the Lyman edge. Variations in the fitting procedure used to derive the effective area curve from the observation (judgments on how smooth the curve should be) lead to only $\pm$5% excursions around the curve we have adopted. Therefore, since the statistical precision is also excellent, if the DA white dwarf model atmosphere is correct, the HUT sensitivity curve is extremely well determined.

Several lines of evidence support the belief that the G191-B2B model flux is accurate to the level cited. A comparison of the observed spectra for G191-B2B and the significantly cooler DA white dwarf HZ43 confirms the self-consistency of the model atmospheres employed (Kimble et al. 1993b). Independent of white dwarf models, a preliminary analysis of the HUT observation of the BL Lac object PKS2155-304 indicates that, when fluxed with the G191-B2B-based calibration, the spectrum is well fitted by a power-law all the way to the Lyman limit, as expected for this object. Finally, the ratio of the in-flight to pre-flight calibrations varies with wavelength by only 20%, and this is in a manner that is consistent with the degradation we have previously observed for detectors of this type. There is thus no reason to suspect any large calibration error of the magnitude that has plagued sub-Lyman-α spectrophotometric observations in the past (see Holberg et al. 1991 and references therein).

For use in the routine reduction of HUT data, the effective area curve is transformed into an inverse sensitivity curve (units $\mathrm{erg\ cm^{-2}\ \AA^{-1}\ count^{-1}}$) which includes the pulse persistence correction of 0.926.

Figure 4-5: Expected first order effective area for Astro-2.

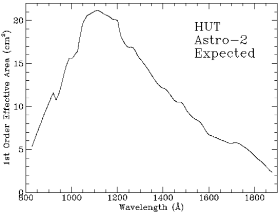

Figure 4-6: Expected second order effective area for Astro-2.

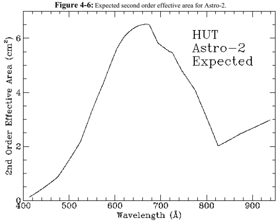

Figure 4-7: Expected second order + Al filter effective area for Astro-2.

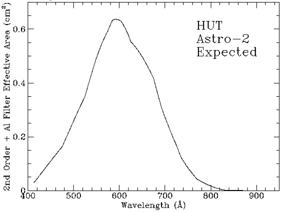

The HUT detector for the flight of Astro-1 used a cesium iodide (CsI) photocathode, the spectrograph grating was coated with osmium, and the primary mirror was coated with iridium. Each of these primary components has been improved for Astro-2 to provide approximately a factor of three overall increase in first-order effective area. The refurbished spectrograph has a silicon carbide (SiC) coating on the grating. The Astro-2 detector also has a fresh CsI photocathode. These two improvements represent a net gain of about 50% in efficiency for the spectrograph and detector system in first order. The flight mirror from Astro-1 has been replaced with the backup mirror, which we have coated with SiC for another factor of two gain in first-order throughput.

The new spectrograph and detector system have been calibrated in the laboratory in our facilities at JHU as well as in the synchrotron beam at SURF. The reflectivity of the newly coated mirror has also been measured in the lab here at JHU and at GSFC. Based on these laboratory calibrations, and including an allowance for degradation of the photocathode efficiency similar to what was seen for Astro-1, we derive the effective area curves shown in Figures 4-5, 4-6, and 4-7. First order effective area peaks near 1200 Å at $\sim 30 cm^2$, and the anticipated effective area for Astro-2 is higher *at all wavelengths* than the *peak* effective area for Astro-1.

Next Up Previous Contents

Next: Photometric Corrections for Image **Up:** CALIBRATION **Previous:** Flat Fields

6/23/1999

Photometric Corrections for Image Motion

Image motion not only shifts the zero point of the spectrum recorded by the HUT detector, but it can also lead to significant loss of light at the edges of the apertures if it is large enough. Since stable pointing was a persistent problem for Astro-1, achieving the highest photometric accuracy requires careful examination of the light lost due to the pointing jitter. We have adopted two approaches to making photometric corrections for image motion. The first relies on the availability of HUT and AST guide stars to explicitly track changes in the pointing direction. The second relies on the statistical distribution of the observed counting rate for an assumed steady source. The latter method is the only recourse for bright stars with no guide stars visible in the HUT TV camera.

The first method starts with the same basic data used to make corrections to the wavelength scale for image motion. To derive a photometric correction, a χ^2 fit is done to the observed counting rate vs. offset position. Using a Gaussian model for the point spread function and an assumed slit profile, we fit the data to determine the slit center, the width of the PSF, and the intensity of the target. Only data from regions free of airglow line emission are used in the fits. The derived intensity from this fit is used to renormalize the flux-calibrated spectrum.

The second method assumes that the observed source is constant in intensity and should only display Poisson fluctuations in the count rate in spectral regions free of airglow lines. A first pass through the data eliminates regions with obviously low count rates when the source is clearly out of the aperture. The high end of the count rate distribution is then fit to a Poisson distribution to determine the best value for the source intensity. In the absence of satisfactory results for photometric corrections based on guide star data, this Poisson-derived count rate is used to renormalize the flux-calibrated spectrum to our best estimate of the true source flux. An obvious shortcoming of this method occurs for observations of targets with reasonably stable pointing that are poorly centered in the aperture -- the count rate may be steady and be a good match to a Poisson distribution, but it may be lower than the true flux. For this statistical method to succeed, the object must spend some time near the aperture center so that the highest count rates observed match the true source intensity. We have increased several of the aperture sizes for Astro-2 compared to those used on Astro-1 to improve the photometric accuracy of the data.

OBSERVATION FEASIBILITY ESTIMATES

Using the calibration information presented in the previous section, we now discuss estimating the feasibility of a variety of possible science observations using HUT. Quick estimates of expected signal-to-noise ratios (S/N) can be made using the sensitivity curves presented in Figures 5-1 and 5-2. These show the continuum flux or surface brightness required to achieve a S/N ratio of 10 per Å in a single 1800 s observation for a point source and for extended sources which fill the long slits. For comparison we show similar sensitivity curves for IUE observations using the SWP camera and the large aperture.

Figure 5-1: Point source sensitivity to achieve S/N = 10 per Å in a typical 1800 s exposure. The dashed curve shows the sensitivity of the IUE SWP for the same assumptions.

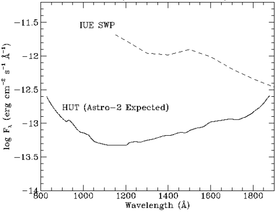

Figure 5-2: Extended source sensitivity to achieve S/N = 10 per Å in a typical 1800 s exposure. Diffuse emission is assumed to fill the apertures indicated. For IUE, the emission is assumed to fill the 10x20 arcsec large aperture.

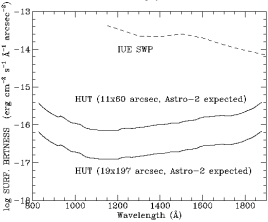

More detailed estimates can be made using the following procedures. For a continuum source, the number of detected counts per ~0.5 Å pixel can be estimated using the anticipated effective area curve presented in Figure 5-4 and the relation

$$N_\lambda = \frac{\lambda F_\lambda}{hc} A_\lambda \Delta t \Delta\lambda \ \text{counts pixel}^{-1}, \quad (1)$$

where F_λ is in $\mathrm{erg\ cm^{-2}\ s^{-1}\ \AA^{-1}}$, A_λ is the effective area (from Figures 4-5, 4-6, or 4-7), Δt is the integration time (typically 1800 s for a single pointing), and $\Delta\lambda =$ 0.51336 Å for first order, or 0.25668 Å for second order.

For an extended source, one must use the surface brightness for F_λ in $\mathrm{erg\ cm^{-2}\ s^{-1}\ \AA^{-1}\ arcsec^{-2}}$ and the angular size $\Delta\Omega$ of either the slit or the source, whichever is smaller, as in

$$N_\lambda \ = \ \frac{\lambda F_\lambda}{hc} A_\lambda \Delta t \Delta\lambda \Delta\Omega \ \ \mathrm{counts\ pixel^{-1}}. \qquad (2)$$

The angular areas of the HUT slits are given in Table 5-1.

=-2 Count rates for continuum sources must be less than 2.5 counts s^{-1} $pixel^{-1}$ and less than 40 counts s^{-1} $pixel^{-1}$ at the peaks of isolated emission lines. For sources with rates in excess of these values, the full aperture of the telescope must be stopped down. Closing one door gives a reduction of a factor of two. The 50 cm^2 small aperture door gives a reduction of a factor of 102, and the 1 cm^2 small aperture door gives a reduction of a factor of 5120. (Use of the 1 cm^2 small aperture door requires special procedures to avoid undue pressure buildup in the telescope and spectrograph due to outgassing. Use of this door state should be avoided if possible.)

Table 5-1: HUT Science Aperture Expected Properties for Astro-2

Aperture	Size[a] (arcsec)	Resolution (Å)	$\Delta\Omega$ ($\mathrm{arcsec^2}$)	Background Rates (10^{-3} counts s^{-1} pix^{-1}) Night	Day
1	12	4	113	0.4	1.0
2	32	12	804	0.8	4.5
3	32	12	804	0.4[b]	0.4[b]
5	19×197	7	3743	2.3	20
6	10×56	4	560	0.6	3.2
7	20	7	314	0.5	2.0

[a]Single numbers denote the diameters of circular apertures. Two numbers refer to rectangular apertures.
[b]Aluminum filter on aperture 3 blocks Lyα.

To evaluate the signal-to-noise ratio (S/N) for a specific observation, one must also take the background into account. The dark count due to charged particle events is quite low, but scattered light from geocoronal Lyα makes a significant contribution to the general background, particularly during orbital day or if large apertures are chosen. For a continuum point source the S/N is given by

$$S/N \ = \ N_\lambda \sqrt{\frac{\Delta t \Delta n}{(N_\lambda + B_\lambda)}}, \qquad (3)$$

where B_λ is the background rate per pixel and Δn is the number of pixels. Table 5-1 also shows the anticipated background rates due to dark counts plus scattered light in each of the HUT science apertures for both orbital day and orbital night. We assume a geocoronal Lyα intensity of 2 kR (1 Rayleigh = $10^6/4\pi$ photons $\mathrm{cm^{-2}\ s^{-1}\ steradian^{-1}}$) during night, and 20 kR during day though the actual values will differ and also depend on the shuttle orbital position and the pointing direction. These are conservative estimates based a flight near solar minimum using the models of Meier (1991).

Discrete airglow lines also substantially increase the background in their immediate vicinity, especially during orbital day. Typical airglow spectra for an 1800 s observation using the 20$''$ aperture are shown in Figures 5-3 and 5-4 for orbital night and orbital day, respectively. Both spectra have been truncated to show the fainter features. In the night spectrum, Lyα peaks off scale at 4500 counts pix^{-1}. In the day spectrum Lyα is off scale at 37,700 counts pix^{-1}, and O I λ1304 peaks at 1100 counts pix^{-1}. Again, these estimates are based on Meier's (1991) models near solar minimum.

While orbital night clearly offers advantages, about half the scheduled observations *must* take place during orbital day. To reserve the lower background of orbital night for the fainter targets, bright point source observations are normally done during the day.

Figure 5-3: The HUT spectrum illustrates the expected airglow for an 1800 s observation through the 20$''$ circular aperture during orbital night on Astro-2. Lyα is off-scale at a peak of 3500 counts pix^{-1}.

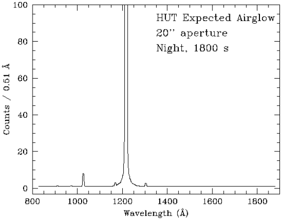

Figure 5-4: The HUT spectrum illustrates the expected airglow for an 1800 s observation through the 20″ circular aperture during orbital day on Astro-2. Lyα and O I λ1304 are off-scale with peaks of 29,300 and 2500 counts pix^{-1}, respectively.

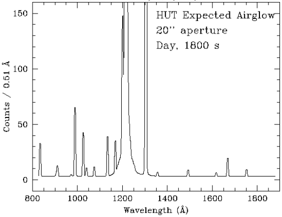

Simulated HUT data for a wide variety of input source spectra can be generated with the HUT simulator `hutsim`, which is a task in the `hut` package in `IRAF`. The following instructions will enable a user to acquire and install a local version of the `hut` package. These instructions are not for a system-wide installation. Rather, the individual user obtains his/her own copy of the programs and files via anonymous `ftp`. Once installed, the package is not visible when starting up `IRAF`, but it can be loaded by typing its name, `hut`.

To install the `IRAF` package `hut` containing the `hutsim` tasks, take the following steps:

1. Change to your `IRAF` directory (where `login.cl` lives).
2. Enter `ftp` and connect to the HUT computer using one of these methods:

   `>ftp hut4.pha.jhu.edu` OR

   `>ftp 128.220.26.36`

3. Enter the userid `anonymous` and your name for the password.
4. Change to the `hutsim` directory, set the transfer mode to binary, use the `get` command to retrieve the `hutsim` tar file, and exit ftp:

   `ftp> cd hutsim`

```
ftp> binary

ftp> get hutsim.tar

ftp> quit
```

5. Run `IRAF` on your machine:

   ```
   >cl
   ```

6. Use the `rtar` task of the `softools` package to expand the tar file:

   ```
   cl> softools

   so> rtar -xvf hutsim.tar

   so> bye
   ```

7. Two new entries will appear:

   README.cl -
   A script file that performs the IRAF installation.
   hut -
   The directory where the `hut` package lives.

8. Use the `page` task to examine the `README.cl` file for further instructions:

   ```
   cl> page README.cl
   ```

9. Once the `hut` package is installed, `hutsim.tar` may be removed. Detailed instructions for using `hutsim` can be obtained by printing the `IRAF help` file using the following procedure:

   ```
   cl> help hut$src/doc/hutsim.hlp file+ page- | lpr
   ```

   (This special procedure is necessary since the help files for the `hut` package are not installed in the system-wide `IRAF` help database.)

MISSION PLANNING

The process of planning a science mission on the space shuttle is a complicated one, especially if ``astronomy'' is the science being pursued. The planning process has to include all the constraints intrinsic to the actual observations (e.g., visibilities of the objects from low-earth orbit, brightness of the objects, position relative to the day/night terminator of the orbit [or the sun or the moon], etc.), as well as all the constraints that arise due to the shuttle itself (e.g., propellant available for maneuvers, maneuver rates, thermal constraints, crew cycles, availability of TDRS coverage for communications, etc.). Even though the three UV telescopes are co-aligned, the science goals of each team are sufficiently different from one another that mechanisms are needed to assure that the resources are shared equitably between the teams. In addition, the actual science programs can cause additional constraints (e.g., ephemeris targets, moving targets, or objects that should only be observed in conjunction with another object, etc.).

Pre-mission planning involves planners from the science teams (including Guest Investigators), the Marshall Space Flight Center Mission Operations Laboratory and the Johnson Space Center Mission Operations Directorate. The science teams are responsible for developing a proposed sequence of observations (science plan) that best accomplishes the science goals of the science teams and their Guest Investigators. This involves selecting and prioritizing potential targets for a given launch assumption (based on target visibilities and science priorities) and then actually building the proposed sequence of observations in detail. Subsequent to this, the MSFC planners take the science plan as an input to create the ``attitude timeline''; orbiter maneuvers are designed to accomplish science pointing needs as well as to satisfy various Orbiter and Spacelab needs. In the mean time, the science team members do all of the background work necessary to ensure a proper instrument configuration for the observation. For HUT this includes selecting the appropriate aperture, choosing potential HUT TV guide stars and magnitude settings, finalizing coordinates or any requested roll angles, estimating the expected count rate for each object, and determining whether any special procedures are necessary, either for instrument safety or for special observational requirements (e.g., offsets, variable targets, etc.). When compiled and verified, this information is translated into a form understandable by the instrument and Spacelab computers and loaded onto the Mass Memory Unit (MMU) on the Shuttle.

The following sections will describe many of these steps in more detail, concentrating on the details of observation planning that are specific to HUT observations. The reader is directed to the Mission Planning Handbook and Interface Requirements Document (MPHIRD) for more detailed information on other aspects of mission planning.

6/23/1999

Selecting Targets for a Given Launch Assumption

Visibility of targets from low earth orbit is dependent on not only the launch time of year, but also on the specific orbital parameters assumed and various planning constraints such as the size of the solar avoidance zone or earth limb-angle viewing constraints. Because launch dates have a way of shifting around unexpectedly in the Shuttle world, it is important to have targets available year round. The list of all potential targets for any time of year is called the Program Target List (PTL); once selected, GI targets will be added to this file as the first step of the planning process. If good 1950 epoch coordinates ($\sim 1''$)are available at this point it will simplify things downstream in the process, although later updates are possible.

When a launch date and time and an assumed orbit are made available, the PTL can be culled down to a list of targets with acceptable visibilities. Science team members (again, including GI's) prioritize this list and assign requested observing times to those objects that are under consideration for observation. The finalized list is called a ``Mission Target List'', or MTL, and this file provides planners with the information necessary to plan a science timeline.

The problem of creating a ``science plan'' (SCIPLAN) boils down to arranging the potential targets into a sequence of observations that are consistent with the target visibilities and all the other constraints arising from other considerations (including STS thermal and communications constraints, for instance). Software has been developed to calculate these visibilities and to insert objects into the observation sequence, checking constraints and leaving time for slews between the various targets. Producing this timeline is no small task and has not been fully automated because of the large number of ``gray'' constraints (i.e., constraints that one might be willing to violate for one target, but not another).

For Astro-2, we intend to modify the ``SCIPLAN'' process to include a concept called ``block scheduling''. The mission will be broken into integral orbit blocks and the blocks will be assigned to the teams in relation to the total time each team (including its GI's) is assigned for the mission. (At present it is envisioned that blocks will be two orbits long.) This is done before the SCIPLAN planning begins. Each team can then plan ``their'' blocks as they desire, and only the block interfaces need to be negotiated. (In reality, recall that each of the three UV telescopes is observing every possible target, so this is really just a planning aid.) As needed during the mission, each team can shuffle or replan their blocks with relative impunity, in order to maximize their instrument's scientific return. HUT GI observations will simply be scheduled in the ``HUT'' blocks, like any other HUT target. Once the SCIPLAN file has been finalized, the MSFC Payload Activity Planner (PAP) team and the instrument teams work in parallel on various activities.

Since the nominal launch plan for Astro-2 calls for a night launch into a 28^{0} inclination circular orbit, to first order, the night visibility of a given target is what one would expect to see from a ground-based observatory at a northern latitude of $+28^{0}$.Many targets can also be effectively observed during orbital daylight. The only daylight targets that are absolutely excluded are those within the 45^{0} solar avoidance zone. Targets within 25^{0} of the moon are also nominally excluded. Targets with substantial amounts of both day and night visibility are classified as ``Night into Day'' or ``Day into Night'', depending upon when they rise sufficiently high above the earth limb. During daylight, targets must be $>10^{0}$ above the earth limb, and during night this constraint is relaxed to 5^{0}.Since only half the available observing time is during orbital night, however, the scheduling strategy tries to preserve orbital night for faint targets or for extended sources, concentrating on bright point sources during orbital day.

While targets near the pole of the shuttle orbit can have nearly continuous visibility, these opportunities are rare since the orbital pole shifts as the earth rotates underneath the shuttle. More typical visibilities are closer to 2000 s, and, once allowance is made for acquisition times, most observations have only 1500-1800 s of actual science data. Maneuver times can also have a substantial impact on the time available for scientific observations, especially if targets are far apart on the sky. The shuttle can slew at 0.2^{0} per s, so the maximum maneuver time is 900 s. Average maneuvers are on the order of 400-600 s. One potential time-saving feature for targets that lie within the 20^{0} maneuvering cone of the IPS is to perform an IPS slew. These are faster (0.5^{0} per s), and they are particularly suitable for clusters of bright sources that require only a few hundred seconds of integration time.

Detailed Observation Planning

6/23/1999

Sequence Database Files

For each potential observation planned in the SCIPLAN file, we create a HUT Sequence Database file. (Multiple observations of a target will have multiple files.) The files are ASCII text in a keyword/entry format that is easy to edit. These files are used for several purposes. They are the receptacles for general information about each target (magnitudes, fluxes, coordinates, references from the literature, etc.), and as such can start to be built (on a target by target basis) even before the SCIPLAN planning takes place. Also, at various stages of the planning process, ``official'' planning information from the MSFC outputs (e.g. roll angles, start and stop times for the planned observations, unique observation ID numbers, etc.) are fed back into the sequence database files to keep them current. Finally, as observation planning progresses, these files hold parameters that reflect the decisions made to set up each observation (selected aperture, guide stars to use, TV magnitude settings, expected count rates, whether special procedures are required, etc.). Most of the information placed in these files is in a fairly ``user-friendly'' format (i.e. magnitudes, guide star positions in arcsec relative to the object position, etc.). When these files are completed and verified, software converts this information into the format needed for operating the telescope on orbit. (For example, the roll angle and guide star offsets [in arcsec] are converted into HUT TV pixel coordinates; this information is used by the HUT DEP to generate fiducial marks on the HUT TV at the expected positions of guide stars.) The transformed files are called ``sequence files'' (as opposed to sequence database files).

Science team members are assigned responsibility for a certain class or number of targets. This responsibility involves checking and verification of information, selection of guide stars, setting of observation and instrument parameters, and calculation of expected count rates. ``Write'' protections are set so that only the person responsible for that observation can edit the file. An exception is that information from MSFC planning files is inserted ``wholesale'' by a superuser who has access to all the files.

Coordinates and Roll Angles

It is important to have accurate coordinates (and accurate relative positions of potential guide stars, if appropriate) for each target or observation. Object coordinates are nominally placed in the PTL file (and get pulled forward into the MTL file), where columns for indicating the accuracy of the coordinate and a reference for the coordinate are also provided. Separate entries in the sequence database files track the coordinates listed on the SCIPLAN and those entered by science planners to assist in the process of checking. However, there are a number of reasons why coordinates may need to be updated at a later stage in the process. For instance, if the coordinate supplied for the PTL was only accurate to 30", a better coordinate is needed for the actual observation (typically 1-2" accuracy). Also, an extended target selected by UIT (which has a 40' field of view) may have a ``generic'' coordinate in the PTL, and the spectrograph observers may choose a specific location for observation. Finally, it is desirable to have the best possible coordinate for any moving targets such as planets or comets, and these are often put in after the SCIPLAN is completed. Whatever the case, selecting, measuring, and/or verifying the coordinates and accuracies is an important step of planning, done shortly after the SCIPLAN is available.

Likewise, if any extended targets require specific roll angles, say to place a rectangular HUT aperture along the major axis of an elliptical galaxy, this needs to be determined and requested so that the orbital analysis engineers at MSFC can find appropriate guide stars for the IPS. Again, there are entries for setting a ``roll requested'' flag and desired roll angle in the MTL file, and the same information needs to get propagated to the sequence database files. However, final decisions on some targets are not made until they are actually planned into the SCIPLAN, so an iteration and verification is usually needed.

Selecting HUT Guide Stars

With the general exception of bright stars (V<10), it will be desirable to select HUT guide stars for most targets. For each guide star (up to three can be selected), fiducial marks will appear on the HUT TV camera at the expected positions. This will assist the payload specialist in identifying the field and quickly centering the correct object in the aperture. In certain cases where an object is too faint to be seen, this is the only way to assure the target is within the aperture. In cases where the object is bright, once the object is placed in the spectrograph aperture, the guide stars can be used to hold it there. Also, error signals for each of the guide stars are generated for use in pointing the telescope and for post-flight analysis.

Most of the leg work in obtaining information on potential guide stars for each object is accomplished by HUT team members who obtain the information from the HST Guide Star Catalog (HSTGSC). While absolute positions from the HSTGSC are sometimes off by as much as several arcsec, the relative positions (say target to surrounding potential guide stars) are typically much better (sub-arcsec). Likewise, magnitude information from the HSTGSC may only be good to $\sim$0.5 mag, but for ``random'' field stars surrounding each target, its the only game in town.

Because the HUT TV camera has limited dynamic range at each of its gain settings, guide stars should not span a range of more than 2.5 magnitudes. In addition, to protect the TV camera, it must be set to accommodate the brightest objects in the field. This requirement leads to the restriction that the target magnitude entered in the sequence database file can be no more than 5 magnitudes fainter than the brightest object in the TV field of view. We must be particularly careful in the region around the entrance slits. When observing bright targets, there is always a chance that they will pop out of the slit area, so the mean guide star magnitude in a sequence database file may not be more than 3 magnitudes fainter than the target.

The HUT TV field of view is roughly $9' \times 12'$. Based on analysis of the HSTGSC data for each object, information on potential guide stars within this region will be entered into each HUT sequence database file. This includes magnitude and relative positional information, and a ``flag'', initially set to ``no'' in all cases, that indicates whether or not the guide star is to be used. The person responsible for each target is tasked with inspecting the field of each object and selecting up to three of the guide stars for actual use during the observation.

Because the HUT TV camera contains small geometric distortions, it is best to select guide stars reasonably close to the target (but >30$''$), and surrounding the target (as opposed to all on one side of the field) whenever possible. Because field rotation angle may make guide stars outside 4.5$'$ radius unavailable, one should choose such stars with caution. Unfortunately, Mother Nature does not always provide ideal situations, and one or two guide stars, or guide stars all on one side of the TV field, are better than no guide stars at all.

Count Rates and Door States

It is important to have some idea of the count rate expected from each target, both for reference during the mission, and for instrument safety considerations. The program `hutsim`, described earlier in this manual, provides a mechanism for simulating spectra of each object and estimating the count rates expected, including airglow lines. (The plots from these simulations can also be placed in the Target Book used by the payload specialists to set up an observation and verify that all is proceeding nominally.)

Sources whose predicted count rates exceed 5000 counts s^{-1} exceed safety limits for the detector. High count rates can also present dead time problems as described earlier in this manual. These situations can be handled in a number of ways. For extended sources, selecting a smaller aperture may resolve the problem. For point sources, however, one may have to choose something other than the full telescope aperture. The flux may be attenuated by a factor of two by closing one or the other of the ``half aperture'' doors at the front of the telescope. If still too bright, the large aperture doors can be closed, and one of two small aperture door positions (50 cm^2 or 1 cm^2) can be utilized. All of these situations can be simulated using `hutsim` in order to both derive expected count rates, and analyze the quality of the data resulting from one of these alternate door states.

APPENDIX A -- LIST OF REFERENCE DOCUMENTS

``Far-Ultraviolet Astronomy on the Astro-1 Space Shuttle Mission,'' A. F. Davidsen, *Science*, **259**, 327, (1993).

The Hopkins Ultraviolet Telescope: Collected Scientific Papers, Vol. I, ed. A. F. Davidsen, (Baltimore: Johns Hopkins University) (January 1993).

``The Hopkins Ultraviolet Telescope: Performance and Calibration During the Astro-1 Mission,'' A. F. Davidsen et al., *Ap. J.*, **392**, 264, (1992).

HUT Dedicated Experiment Processor Software Requirements Document, Rev. E, J. R. Dettmer & B. Ballard, (Laurel: Johns Hopkins University Applied Physics Laboratory) (April 1990).

``An Intensified Photo Diode Array Detector for Space Applications,'' K. S. Long, C. W. Bowers, P. D. Tennyson, and A. F. Davidsen, *Advances in Electronics and Electron Physics*, **64A**, 239, (1985).

Mission Planning Handbook and Interface Requirements Document (MPHIRD), W. P. Blair et al., (Huntsville: Marshall Space Flight Center) (April 1993).

``Ultraviolet Spectroscopy and Remote Sensing of the Upper Atmosphere,'' R. R. Meier, *Space Science Rev.*, **58**, 1, (1991).

APPENDIX B -- LIST OF ACRONYMS

A/D	Analog-to-digital
A/G	Air-to-ground
AOS	Acquisition of signal
AST	ASTROS Star Tracker
ASTROS	Advanced Star/Target Reference Optical Sensor
CCTV	Closed-circuit television
CsI	Cesium Iodide
DDU	Digital Display Unit
DEP	Dedicated Experiment Processor
EC	Experiment Computer
ECC	Environmental Control Cannister
ECAS	Experiment Computer Applications Software
ECOS	Experiment Computer Operating System
EM	Electronics Module
FHST	Fixed-head Star Tracker
FWHM	Full-width half-maximum
GI	Guest Investigator
GSE	Ground Support Equipment
HAC	HUT Activation
HDC	HUT Doors and Camera
HMH	HUT Mirrors and Heaters
HOP	HUT Operations
HRM	High-rate Multiplexer
HSP	HUT Spectrometer
HST	Hubble Space Telescope
HSTGSC	HST Guide Star Catalogue
HUT	Hopkins Ultraviolet Telescope
ID	Identification
IDIN	Identification Initial
IDOP	Identification Operational
IMC	Image Motion Compensation
IMCS	Image Motion Compensation System
IPS	Instrument Pointing System

IRAF	Interactive Reduction and Analysis Facility
IRS	Integrated Radiator System
ISM	Interstellar medium
IUE	International Ultraviolet Explorer
JPL	Jet Propulsion Laboratory
JSC	Johnson Spaceflight Center
LOS	Loss of signal
LOT	Lock on target
MCP	Microchannel plate
MMU	Mass Memory Unit
MPHIRD	Mission Planning Handbook and Integration Requiements Document
MS	Mission Specialist
MSFC	Marshall Spaceflight Center
MTL	Mission Target List
NIST	National Institute of Standards and Technology
OCR	Operation Change Request
OMIS	Operation Managment Information System
OSP	Optical Sensor Package
OSPCAL	Optical Sensor Package Calibration
PAP	Payload Activity Planner
PATSI	Problem analyst and trouble-shooting investigator
PI	Principal Investigator
POCC	Payload Operations Control Center
PP	Peripheral Processor
PS	Payload Specialist
PSF	Point spread function
PTL	Program Target List
RAM	Random Access Memory
RAU	Remote Acquisition Unit
RR	Replanning Request
S/N	Signal-to-noise ratio
S/W	Software
SCIPLAN	Science Plan
SIT	Silicon Integrating Target
SOPG	Science Operations Planning Group
SP	Spectrometer Processor
STS	Space Transportation System
SURF	Synchrotron Ultraviolet Radiation Facility
SWP	Short wavelength prime
SiC	Silicon carbide
TDRS	Tracking and Data Relay Satellite
TEGSE	Telemetry experiment ground support equipment
TM	Telescope Module
UIT	Ultraviolet Imaging Telescope
UV	Ultraviolet
WUPPE	Wisconsin Ultraviolet Photopolarimeter Experiment

6/23/1999

About this document ...

This document was generated using the **LaTeX**2HTML translator Version 97.1 (release) (July 13th, 1997)

The command line arguments were:
latex2html `hut_handbook.tex`.

The translation was initiated by on 6/23/1999

6/23/1999

...assumption

Because of our experience with launch slips and near-launches on Astro-1, launch dates and times are referred to as ``launch assumptions'' until such time as they actually occur.

6/23/1999